Theoretical Study of Substituent Effects in the Diimine−M(II) Catalyzed Ethylene Polymerization Reaction Using the IMOMM Method

Robert D. J. Froese, Djamaladdin G. Musaev,* and Keiji Morokuma*

Contribution from the Cherry L. Emerson Center for Scientific Computation and Department of Chemistry, Emory University, Atlanta, Georgia 30322

Received August 13, 1997. Revised Manuscript Received December 2, 1997

Abstract: The integrated molecular orbital−molecular mechanics (IMOMM) method adopting the B3LYP:MM3 combination has been used to study the full catalysts in the diimine−M (M = Ni, Pd) catalyzed ethylene polymerization reaction. These results have been compared with previous molecular orbital calculations on model systems (model). There is a lowering of the migratory insertion activation barriers when including substituent effects from 9.9 (model) to 3.8 (IMOMM) kcal/mol for nickel and from 16.2 (model) to 14.1 (IMOMM) kcal/mol for palladium. Steric interactions decrease the complexation energy which leads to a lowering of the barrier. The β-H transfer process which involves the reaction *n*-propyl β-agostic → olefin hydride → isopropyl β-agostic is the likely mechanism leading to branching of polyethylenes. In the nickel system, the olefin−hydride intermediate lies 13.6 (model) or 14.5 (IMOMM) kcal/mol above the *n*-propyl β-agostic species, indicating that this pathway is unlikely for unsubstituted or substituted nickel diimine catalysts. For palladium, where the olefin−hydride intermediate resided 5.4 kcal/mol above the β-agostic species in model B3LYP predictions, IMOMM reduces this difference to almost zero, suggesting branching to be more prominent with bulky substituents. Although β-H transfer is more likely for substituted palladium, the formation of the 5-coordinate intermediate is not possible due to steric effects and thus an associative chain termination process is not possible for substituted palladium while it likely can occur for unsubstituted Pd catalysts.

1. Introduction

Transition metal catalyzed olefin polymerization reactions are an important process to the chemical industry and have been a focus of chemists in recent years.[1−3] Both the experimental and theoretical studies of these systems are of fundamental and practical consequence by controlling the polymer microstructure and molecular weight. In one sense, these studies can be divided into two distinct classes: (1) the adjustment of ligand, cocatalyst, solvent, and metal in an effort to improve the existing technology[1,2] and (2) the search for more active alternative catalysts.[2c,4]

Recently, a series of theoretical papers dealing with ethylene polymerization using nickel,[5] palladium,[6] and platinum[7] diimine catalysts has been published and compared with experimental data.[4] These papers study the initiation step and the propagation step, as well as many chain termination processes, in ethylene polymerization. Many interesting features of this class of catalysts have been documented experimentally.[4] First, the diimine−M(II)−alkyl cation with bulky diimine ligands ArN═C(R)C(R)═NAr, where Ar = 2,6-C_6H_3(*i*-Pr)$_2$ and 2,6-$C_6H_3Me_2$ and R = H and Me, is the active species of the polymerization reaction. For palladium, if the bulky ligands are not present (as in the unsubstituted diimine−M−alkyl complex, where diimine is [HN═C(R)C(R)═NH] and R = H and CH_3), the reaction with the olefin leads mainly to dimerization or oligomerization, but not to the polymerization observed when the bulky ligands are present. The polyethylene produced by M = Pd substituted catalysts shows extensive branching along the main chain with the branches being distributed randomly and having various lengths. In contrast, polyethylene produced by Ni(II) catalysts ranges from highly linear to moderately branched, with methyl branches predominating. A variety of factors control the branching, including temperature, ethylene pressure, and catalytic structure. If the temperature is increased, branching is increased, while higher ethylene pressure promotes a decrease in the branching ratio. If the steric bulk of the diimine ligand is reduced, more linear polymers with decreased molecular weights are found. Finally and very importantly, it was shown that the nickel catalyst has an activity near that of

(1) Thayer, A. M. *Chem. Eng. News* **1995** (Sept 11), 15.

(2) As leading references, see: (a) Huang, J.; Rempel, G. L. *Prog. Polym. Sci.* **1995,** 20, 459 and references therein. (b) Coates, G. W.; Waymouth, R. M. *Science* **1995**, 267, 217. (c) van der Linden, A.; Schaverien, C. J.; Meijboom, N.; Ganter, C.; Orpen, A. G. *J. Am. Chem. Soc.* **1995**, *117*, 3008. (d) Yang, X.; Stern, C. L.; Marks, T. J. *J. Am. Chem. Soc.* **1994**, *116*, 10015. (e) Coughlin, E. B.; Bercaw, J. E. *J. Am. Chem. Soc.* **1992**, *114*, 7606. (f) Crowther, D. J.; Baenziger, N. C.; Jordan, R. F. *J. Am. Chem. Soc.* **1991**, *113*, 1455. (g) Kaminsky, W.; Kulper, K.; Brintzinger, H. H.; Wild, F. R. W. P. *Angew. Chem., Int. Ed. Engl.* **1985**, *24*, 507. (h) Ewen, J. A. *J. Am. Chem. Soc.* **1984**, *106*, 6355.

(3) As leading reference, see: (a) Yoshida, T.; Koga, N.; Morokuma, K. *Organometallics* **1995**, *14*, 746. (b) Yoshida, T.; Koga, N.; Morokuma, K. *Organometallics* **1996**, *15*, 766. (c) Woo, T. K.; Fan, L.; Ziegler, T. *Organometallics* **1994**, *13*, 2252. (d) Fan, L.; Harrison, D.; Woo, T. K.; Ziegler, T. *Organometallics* **1995**, *14*, 2018. (e) Lohrenz, J. C. W.; Woo, T. K.; Ziegler, T. *J. Am. Chem. Soc.* **1995**, *117*, 12793. (f) Hyla-Kryspin, I.; Niu, S.; Gleiter, R. *Organometallics* **1995**, *14*, 964.

(4) Johnson, L. K.; Killian, C. M.; Brookhart, M. *J. Am. Chem. Soc.* **1995**, *117*, 6414.

(5) Musaev, D. G.; Froese, R. D. J.; Svensson, M.; Morokuma, K. *J. Am. Chem. Soc.* **1997**, *119*, 367.

(6) Musaev, D. G.; Svensson, M.; Morokuma, K.; Strömberg, S.; Zetterberg, K.; Siegbahn, P. E. M., *Organometallics* **1997**, *16*, 1933.

(7) Musaev, D. G.; Froese, R. D. J.; Morokuma, K. *New J. Chem.* **1997**, *21*, 1269.

S0002-7863(97)02833-3 CCC: $15.00
Published on Web 02/05/1998

metallocenes and is much more active than its palladium analogue.

In our previous theoretical papers,[5−8] we used the unsubstituted system as a model for the real system. We believe that a comparison of the energetics of the initiation pathway and important points on the chain termination pathways for the "real" catalyst with bulky ligands using the newly developed integrated molecular orbital−molecular mechanics (IMOMM) procedure[9] with the corresponding values from our previous model studies can help to determine the effect of these bulky substituents on the polymerization process. In a separate paper, the IMOMM method has been used on these diimine systems to examine the relative stability of the 5-coordinated species with and without substituents.[8] In the present paper, we apply this integrated approach to the two reactions. The first of them is the polymer chain initiation reaction

$$[L_2MCH_3]^+ + C_2H_4 \rightarrow [L_2MCH_2CH_2CH_3]^+ \qquad (1)$$

which, according to the Cossee mechanism,[10] includes the addition of an olefin to the diimine−metal−alkyl cation to form the olefin−alkyl complex and the migratory insertion of the olefin into the metal−alkyl bond via the four-center transition state leading to the γ-agostic intermediate. This species can rearrange into the more stable β-agostic intermediate traversing a rotational transition state with a small barrier.

The second reaction studied in this paper is the β-H elimination chain termination reaction:

$$[L_2MCH_2CH_2CH_3]^+ \rightarrow [L_2M(H)(CH_2{=}CHCH_3)]^+ \rightarrow [L_2MH]^+ + CH_2CHCH_3 \quad (2)$$

This highly endothermic process begins from the β-agostic structure, passes through an olefin−hydride intermediate resulting from the activation of the β-hydrogen, and leads to dissociative displacement. Note that the olefin−hydride intermediate is an important metastable structure on the potential energy surface, and from this point, the reaction may split into several different pathways, which were discussed in our previous papers.[5−8] One of them is the approach of another ethylene molecule to the olefin−hydride intermediate to form a 5-coordinate species, which could result in chain termination for the original polymer. Due to the importance of this associative displacement chain termination process, this step has been examined separately at both MO and IMOMM levels.[8] Another path corresponds to the rotation of the olefin forming an isopropyl β-agostic species which leads to branched polyethylene. This path will not studied in this paper.

Thus, in this paper, we will focus on providing new insight based on the IMOMM results on the initiation (eq 1) and β-H elimination (eq 2) reactions and compare these two reactions along with the associative displacement chain termination mechanism from our previous paper.[8]

2. Computational Methods

Geometries and energies of the reactants, intermediates, transition states, and products are calculated using the integrated molecular orbital−molecular mechanics (IMOMM) method.[9] In this integrated method, the energy of the system of interest, the "real system", is represented by a sum of the MO energy of a smaller "model system" and the MM energy (excluding the part taken into account in the MO energy, to avoid double counting) of the "real system". In the present calculation, all active atoms including the incoming olefin and M−CH_3 as well as the unsubstituted diimine [HN═C(H)C(H)═NH] ligand were included in the "model system", which has been treated by the pure MO method. The "real system" includes the real diimine ArN═C(R)C(R)═NAr, where Ar = 2,6-C_6H_3(*i*-Pr)$_2$ and R = Me, in place of the unsubstituted diimine in the "model system". For the MO part, the gradient-corrected hybrid density functional theory B3LYP[11] was used, which has been shown to predict quite reliable geometries and energies.[12] In these calculations, we mainly used the basis set which includes a double-ζ valence basis set, {8s5p5d}/[3s3p2d] and {5s5p4d}/[3s3p2d], with the relativistic ECP (only for Pd) by Hay and Wadt[13] replacing core electrons up to 2p and 3d for Ni and Pd, respectively, and a double-ζ quality basis set of Huzinaga and Dunning[14] for the active part, i.e. the C and H atoms of the alkyl groups and olefins, as well as the standard 3-21G basis set[15] for the N, C, and H atoms of the HN═C(R)C(R)═NH ligand. We have shown previously[6] that larger basis sets did not change the results significantly for the model system. For the MM part, the MM3 force field[16] without the electrostatic contribution was used. The van der Waals parameters reported by Rappe et al. are used for the metal atoms,[17] while all torsional contributions associated with dihedral angles involving metal atoms are set to zero. Other MM contributions involving the metal are set to zero in the IMOMM method, and no additional parameters are used. By adopting R═H and Ar═H as the common model system, we have fixed the N−H and C−H (set 2) bond lengths at the optimized values for pure MO calculation for the model system and the N−C(Ar) and C−C(Me) (set 3) bond lengths at 1.45 and 1.51 Å, respectively. Calculations were performed using our own IMOMM program[9] which contains modified MM3(92)[16] and modified Gaussian-92/DFT[18] programs. All structures were optimized without symmetry constraints. To benchmark the IMOMM predictions, we also performed single-point pure B3LYP MO calculations at the IMOMM-optimized geometries. Thus, we will be comparing all structures at three different levels: the pure MO geometry optimization and energy calculation for the model system (model MO//MO), the IMOMM geometry optimization and energy calculation for the real system (real IMOMM//IMOMM), and the single-point pure MO calculation at the IMOMM-optimized geometries for the real system (real MO//IMOMM).

(8) Musaev, D. G.; Froese, R. D. J.; Morokuma, K. *Organometallics*. Submitted.

(9) Maseras, F.; Morokuma, K. *J. Comput. Chem.* **1995**, *16*, 1170.

(10) (a) Cossee, P. *J. Catal.* **1964,** *3*, 80. (b) Arlman, E. J.; Cossee, P. *J. Catal.* **1964,** *3*, 99.

(11) (a) Becke, A. D. *Phys. Rev. A* **1988**, *38*, 3098. (b) Lee, C.; Yang, W.; Parr, R. G. *Phys. Rev. B* **1988**, *37*, 785. (c) Becke, A. D. *J. Chem. Phys.* **1993**, *98*, 5648.

(12) (a) Musaev, D. G.; Morokuma, K. *J. Phys. Chem.* **1996**, *100*, 6509. (b) Erikson, L. A.; Pettersson, L. G. M.; Siegbahn, P. E. M.; Wahlgren, U. *J. Chem. Phys.* **1995**, *102*, 872. (c) Ricca, A.; Bauschlicher, C. W., Jr. *J. Phys. Chem.* **1994**, *98*, 12899. (d) Heinemann, C.; Hertwig, R. H.; Wesendrup, R.; Koch, W.; Schwarz, H. *J. Am. Chem. Soc.* **1995**, *117*, 495. (e) Hertwig, R. H.; Hrusak, J.; Schroder, D.; Koch, W.; Schwarz, H. *Chem. Phys. Lett.* **1995,** *236*, 194. (f) Schroder, D.; Hrusak, J.; Hertwig, R. H.; Koch, W.; Schwerdtfeger, P.; Schwarz, H. *Organometallics* **1995**, *14*, 312. (g) Fiedler, A.; Schroder, D.; Shaik, S.; Schwarz, H. *J. Am. Chem. Soc.* **1994**, *116*, 10734. (h) Fan, L.; Ziegler, T. *J. Chem. Phys.* **1991**, *95*, 7401. (i) Berces, A.; Ziegler, T.; Fan, L. *J. Phys. Chem.* **1994**, *98*, 1584. (j) Lyne, P. D.; Mingos, D. M. P.; Ziegler, T.; Downs, A. J. *Inorg. Chem.* **1993**, *32*, 4785. (k) Li, J.; Schreckenbach, G.; Ziegler, T. *J. Am. Chem. Soc.* **1995**, *117*, 486.

(13) (a) Hay, P. J.; Wadt, W. R. *J. Chem. Phys.* **1985**, *82*, 299. (b) Wadt, W. R.; Hay, P. J. *J. Chem. Phys.* **1985**, *82*, 284.

(14) (a) Dunning, T. M., Jr. *J. Chem. Phys.* **1971**, *55*, 716. (b) Dunning, T. M., Jr. *J. Chem. Phys.* **1970**, *53*, 2823.

(15) Binkley, J. S.; Pople, J. A.; Hehre, W. J. *J. Am. Chem. Soc.* **1980**, *102*, 939.

(16) (a) MM3(92): Quantum Chemistry Program Exchange, Indiana University, 1992. (b) Aped, A.; Aligner, N. L. *J. Am. Chem. Soc.* **1992**, *114*, 1.

(17) Rappe, A. K.; Casewit, C. J.; Colwell, K. S.; Goddard, W. A., III; Skiff, W. M.; *J. Am. Chem. Soc.* **1992**, *114*, 1.

(18) Gaussian 92/DFT, Revision F.2: Frisch, M. J.; Trucks, G. W.; Schlegel, H. B.; Gill, P. M. W.; Johnson, B. G.; Wong, M. W.; Foresman, J. B.; Robb, M. A.; Head-Gordon, M.; Replogle, E. S.; Gomperts, R.; Andres, J. L.; Raghavachari, K.; Binkley, J. S.; Gonzalez, C.; Martin, R. L.; Fox, D. J.; Defrees, D. J.; Baker, J.; Stewart, J. J. P.; Pople, J. A. Gaussian, Inc., Pittsburgh, PA, 1993.

Table 1. Relative Energies (kcal/mol) for M = Ni for the Initiation and the β-H Transfer Processes in the MO//MO Calculation for the Model System and the IMOMM//IMOMM and MO//IMOMM Calculations for the Real System[a]

		real		
structures	model MO	IMOMM	MM part	real MO
reactant + ethylene	0.0	0.0	0.0	0.0
π-complex	−27.9	−20.4	4.7	−14.3
transition state	−18.0	−16.6	1.2	−11.1
γ-agostic *n*-propyl	−33.3	−30.4	2.2	−25.7
β-agostic *n*-propyl	−39.3	−41.2	−1.9	−36.1
propylene−hydride	−25.7	−26.7	−1.1	−20.7
β-agostic isopropyl	−40.8	−34.7	4.9	−28.5
hydride + propylene	12.9	15.0	2.0	11.9

[a] The MM steric energies in the IMOMM calculations are also included.

Table 2. Relative Energies (kcal/mol) for M = Pd for the Initiation and the β-H Transfer Processes in the MO//MO Calculation for the Model System and the IMOMM//IMOMM and MO//IMOMM Calculations for the Real System[a]

		real		
structures	model MO	IMOMM	MM part	real MO
reactant + ethylene	0.0	0.0	0.0	0.0
π-complex	−31.7	−29.8	1.8	−26.4
transition state	−15.5	−15.7	0.0	−12.5
γ-agostic *n*-propyl	−31.8	−33.6	−1.9	−31.3
β-agostic *n*-propyl	−37.4	−36.2	0.6	−31.6
propylene−hydride	−32.0	−36.0	−3.6	−32.8
β-agostic isopropyl	−39.4	−36.7	2.3	−31.9
hydride + propylene	9.9	7.6	0.3	3.5

[a] The MM steric energies in the IMOMM calculations are also included.

3. Chain Initiation Reaction

Model Catalysts. Previously, the initiation reaction has been examined for the model systems of the unsubstituted diimine nickel and palladium catalysts. The energies obtained are presented in the "model MO" column of Tables 1 and 2, respectively. To briefly summarize, the methylated nickel cation, the active catalyst, binds to ethylene by 27.9 kcal/mol to form a complex and then requires 9.9 kcal/mol to go over the transition state for olefin insertion leading eventually to the β-agostic intermediate which lies 39.3 kcal/mol below the reactants. Ethylene binds stronger at 31.7 kcal/mol, and the activation barrier is larger at 16.2 kcal/mol for Pd than for Ni, leading to the β-agostic intermediate lying 37.4 kcal/mol below the reactants. These results suggest that the diimine nickel catalyst should be more active than palladium, in agreement with experiment.[4] The energetics also suggest that the transition state for Ni should be earlier than that for Pd. This is seen in the optimized geometries of the transition state for the model system, given in parentheses in Table 3; the length of the C−C double bond in the transition state for the nickel catalyst is by 0.025 Å shorter than in the palladium catalyst.

Structure of the Real Catalysts. The IMOMM-optimized geometries of the reactant, perpendicular π-complex, transition state, and γ-agostic species for the real system with substituted diimine are depicted in Figure 1 for Pd. Important optimized bond distances near the reacting center are given in Table 3 for these species for both nickel and palladium and are compared with those (in parentheses) of the unsubstituted model system obtained by pure MO optimizations. Overall, there were no major geometric changes in this initiation pathway, although some subtle but important changes were seen in the π-complex and the transition state. In fact, for the methylated reactant, the model and real geometries do not change substantially for either M = Ni or Pd; for the bond lengths given in Table 3, the largest difference is only 1.5% for one of the Pd−N bond lengths. This small difference between the model and the real geometries is not surprising for the reactant where the steric effects should small.

For the perpendicular π-complex, the M−C$^{\pi}$ bond lengths have not changed significantly on going from the model to the real system. However, the symmetric structure found for the model MO calculations is now slightly asymmetric due to the presence of the isopropyl (*i*-Pr) groups on the phenyl rings. Initially, these *i*-Pr groups were chosen to reside as far away from the reacting center as possible, but some rotated to search for a lower energy local minimum. For nickel, the symmetric model Ni−C$^{\pi}$ bond lengths of 2.175 Å have changed to 2.163 and 2.167 Å in the real catalyst, while for palladium, these lengths of 2.278 Å in the model are 2.285 and 2.322 Å in the real catalyst.

The important parameters for the transition state and the π-complex are the C═C and M···CH_2CH_2 bond distances. For nickel, in the real system compared in the model system, the C═C double-bond distance is at the π-complex longer by 0.003 Å, while the distance at the transition state is shorter by 0.011 Å. Correspondingly, the M···C bond distance at the π-complex is shorter by 0.008 Å, while the distance at the transition state is 0.029 Å longer. The transition state for this exothermic process becomes earlier and the barrier is expected to become smaller on going from the model to the real system for the nickel catalyst. On the other hand, for palladium, the C−C distance is 0.003 and 0.004 Å shorter in the real system than in the model system at the π-complex and transition state, respectively. The M−C distance is longer by 0.044 and 0.011 Å in the real system than in the model system, at the π-complex and transition state, respectively. Thus, we would not expect a significant change in the location of transition state or the barrier height between the heavily substituted real catalyst and the unsubstituted model catalyst.

In the direct product, the γ-agostic species, the important bond lengths of the active region do not change significantly between the real and the model system. For example, the C$^{\alpha}$−C$^{\beta}$ (i in Table 3) and C$^{\beta}$−C$^{\gamma}$ (g in Table 3) bond lengths of the real system differ only up to 0.004 Å from those of the model system both for Ni and Pd.

Energetics for the Real Catalysts. The calculated energetics for the initiation process for both the real and model catalysts are collected in Tables 1 and 2, as well as Figure 2, for Ni and Pd, respectively. All energies in this table are relative to the separated reactants, the methylated cation and ethylene, and include those with the pure MO calculation for the unsubstituted model system (listed as "model MO"), the IMOMM calculation for the substituted real system ("real IMOMM"), and the pure MO calculation for the real system at the IMOMM optimized structures ("real MO"). The IMOMM energy, by definition, is represented as the sum of the MO energy of the model system and the MM energy (steric energy from the MM3 force field) for the real system, the latter being shown explicitly as the "MM part" in Table 1.

First, we will compare for the real system the IMOMM energies with the pure MO energies in Tables 1 and 2, in an effort to benchmark our IMOMM results. For both nickel and palladium, there appears to be systematic differences between the two methods. For nickel, the pure MO method gives higher relative energy by 6.1 (π-complex), 5.5 (transition state), and

Table 3. Optimized Bond Lengths (Å) for the Structures in the Initiation Process in Figure 1: Reactant, π-Complex, Transition State, and γ-Agostic Intermediate[a]

		reactant		π-complex		transition state		γ-agostic *n*-propyl	
		Ni	Pd	Ni	Pd	Ni	Pd	Ni	Pd
a	M−N	1.984 (2.005)	*2.168 (2.200)*	2.045 (2.028)	*2.214 (2.214)*	1.945 (1.923)	*2.102 (2.087)*	1.888 (1.872)	*2.049 (2.044)*
b	N═C	1.294 (1.291)	*1.292 (1.289)*	1.296 (1.290)	*1.291 (1.288)*	1.298 (1.294)	*1.296 (1.290)*	1.301 (1.294)	*1.296 (1.291)*
c	C−C	1.495 (1.486)	*1.495 (1.480)*	1.490 (1.479)	*1.498 (1.482)*	1.484 (1.474)	*1.493 (1.477)*	1.490 (1.476)	*1.496 (1.479)*
d	N═C	1.297 (1.292)	*1.298 (1.289)*	1.297 (1.291)	*1.294 (1.288)*	1.298 (1.292)	*1.293 (1.290)*	1.295 (1.292)	*1.292 (1.288)*
e	M−N	1.873 (1.868)	*2.057 (2.038)*	1.951 (1.925)	*2.107 (2.100)*	1.982 (1.980)	*2.167 (2.176)*	2.003 (2.025)	*2.209 (2.226)*
f	M−Me	1.872 (1.877)	*2.019 (2.019)*	1.928 (1.926)	*2.049 (2.044)*	2.048 (2.063)	*2.228 (2.231)*		
g	C−Me					2.153 (2.221)	*2.123 (2.111)*	1.565 (1.567)	*1.565 (1.566)*
h	M−C			2.163 (2.175)	*2.285 (2.278)*				
i	C−C			1.385 (1.382)	*1.387 (1.390)*	1.411 (1.422)	*1.436 (1.440)*	1.534 (1.534)	*1.531 (1.535)*
j	M−C			2.167 (2.175)	*2.322 (2.278)*	1.995 (1.966)	*2.082 (2.071)*	1.911 (1.907)	*2.037 (2.035)*

[a] For each species, the parameters are in the order of M = Ni for the real system and for the model system (in parentheses) and for M = Pd (in italics) for the real and the model system (in parentheses).

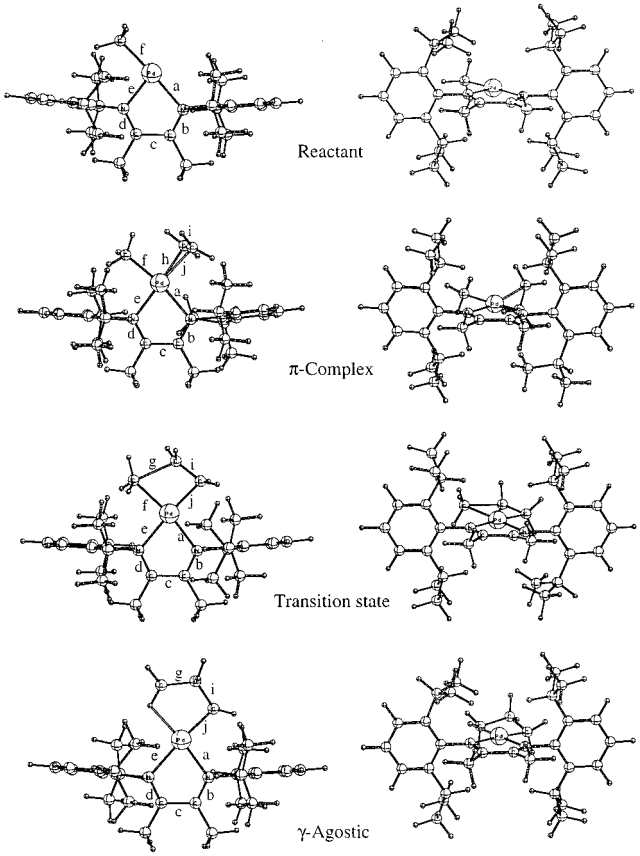

Figure 1. Two views of the structures of the reactant, π-complex, transition state, and γ-agostic intermediates in the initiation process of ethylene polymerization with the substituted "real" diimine Ni and Pd catalysts. The structures depicted are for the Pd system at the IMOMM level. The distances of the labeled bonds are shown in Table 3.

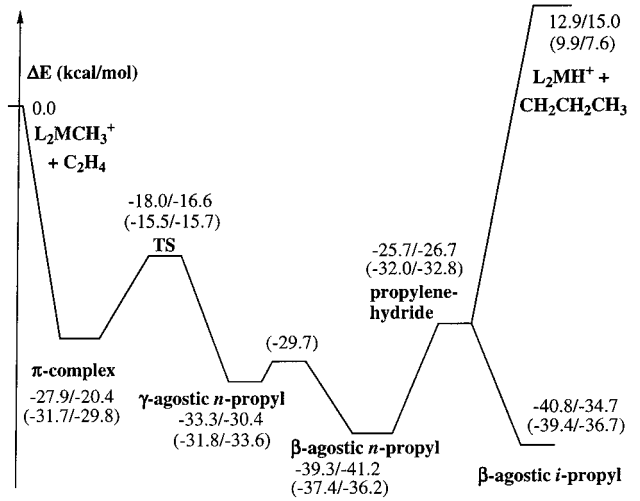

Figure 2. Schematic representation of the relative energies of the reaction of $[L_2MCH_3]^+$ with ethylene for M = Ni and Pd (in parentheses), and for the "model" catalyst (L_2 = [HN═C(H)C(H)═NH], before slash) and the "real" catalyst (L_2 = [ArN═C(Me)C(Me)═NAr], Ar = 2,6-C_6H_3(*i*-Pr)$_2$, after slash).

4.7 (γ-agostic) kcal/mol than the IMOMM method. This means that, if one takes the π-complex as the reference, the energies of the transition state and the product agree within 1.4 kcal/mol between the pure MO and IMOMM method. For the isomers for the β-H elimination pathway in the second half of Table 1, to be discussed shortly, the same trend is seen. The exceptions are the methyl−Ni reactant + ethylene and the hydrido−Ni intermediate + propylene. It appears that the IMOMM method does not stabilizeing the separated reactant or product to the same extent as the pure MO method does. By treating the substituents with the MM force field, the electronic effect of the substituents is missing in the IMOMM method. The lack of electron-donating capability in the MM substituent is suspected of making the coordinatively unsaturated species less stable than they should be. This same trend is also seen for palladium, although not quite as significant; the π-complex, transition state, and γ-agostic species are higher using the MO method by 3.4, 3.2, and 2.3 kcal/mol, respectively. We may conclude that, although there is a slight discrepancy between reactants/products and intermediates/transition states, the barrier heights from the prereaction complex is insensitive between the pure MO and the IMOMM method. Therefore, we can use the IMOMM energies in our comparisons, as the IMOMM method provides separately the steric energy contribution, which is valuable for qualitative discussion.

Next, we will compare the heavily substituted real system (IMOMM) and the unsubstituted model system (pure MO). From Tables 1 and 2, as well as Figure 2, it may seem unusual that some systems have less steric energy than the seemingly smallest and less sterically encumbered system, the methylated reactant. Because of this small ligand, there is a close approach of the methyl hydrogens with those of the outer MM part. In fact, using nickel as an example, there is an approach of two hydrogens of the methyl group to within 2.25 Å of MM atoms, which is closer than any model MO to real MM bond lengths in, for example, the propylene hydride, which has less steric energy. Starting from the reactant for the Ni catalyst, the π-complex is destabilized significantly by 7.5 kcal/mol in the real system. There is 4.7 kcal/mol more steric energy associated

with the π-complex, indicating how much more sterically encumbered this species is. In the calculation of the model system, two π-complexes were actually located, the parallel and the perpendicular, with the perpendicular one, shown in Table 1, being significantly lower by 6.3 kcal/mol. Using the IMOMM method we also located in the real system two π-complexes, with the preference of the perpendicular reduced to 2.5 kcal/mol (IMOMM). In the real system, the steric repulsion due to the bulky substituents reduces the stability of the prereaction π-complex, in particular, the intrinsically more stable and thus more important perpendicular complex. In the transition state, the steric energy is reduced to 1.2 kcal/mol, since the important inserting atoms are now coplanar. The overall effect of the bulky substituents in the real system is therefore to reduce the activation barrier height from 9.9 kcal/mol in the model system to 3.8 kcal/mol. The main reason for this lowering is the 7.5 kcal/mol destabilization of the π-complex, which has been shown before to significantly contribute to lowering of migratory insertion barriers.[7] Of the 6.1 kcal/mol reduction of the barrier, the IMOMM calculation attributes 3.5 kcal/mol to the relaxation of the steric energy at the transition state. Since the structures of the π-complex and the transition state are fully optimized, the optimized geometrical parameters discussed above reflect these energetics.

For the palladium catalyst, the π-complex in the real system is also less stable, compared to the model system, but in this case only by 1.9 kcal/mol. With the palladium atom being larger and the metal−ligand distances longer, the interacting ethylene and the substituents on the diimine are further away from each other and there is less steric repulsions. The steric energy of 1.8 kcal/mol and the symmetric nature of the π-complex in the palladium catalyst compared with 4.7 kcal/mol and the slightly asymmetric nature of the nickel π-complex are indicative of this effect. The activation barrier for the real palladium system is only 2.1 kcal/mol lower than the unsubstituted system.

Thus, the above presented comparisons of the energetics of the polymer chain initiation reaction 1 for the "model" and "real" systems indicate that the activation barrier is lowered with bulky substituents. The main reason for this is destabilization of the π-complex due to steric interactions between the olefin molecule and the bulky substituents. This effect is much larger for diimine−Ni complexes than its Pd analogues because of the difference in the size of the transition metal centers.

4. β-Hydride Transfer Reaction

Model Catalysts. The β-H transfer pathway has previously been examined for the unsubstituted model nickel and palladium catalysts.[5−8] These results are presented in the lower half of Tables 1 and 2, respectively, where the β-agostic *n*-propyl species, the propylene−hydride complex, and another β-agostic species, the isopropyl complex, are presented. To briefly summarize those results, β-H activation for nickel requires a barrier of at least 13.6 kcal/mol since this value is the energy of the propylene−hydride intermediate above the β-agostic *n*-propyl species. The transition state is very difficult to find as it is very similar to the propylene−hydride intermediate both in structure and energy. For palladium, the olefin hydride lies only 5.4 kcal/mol above reactants, with a barrier at the transition state of 5.9 kcal/mol (not shown in Table 2). For both metals in the present discussion, we will consider the propylene−hydride intermediate as the transition state for β-H transfer pathway. Since this pathway leads to the β-agostic isopropyl species, the easier this pathway can be followed, the larger the likelihood of branching. These results suggest that palladium should lead to more branching than nickel.

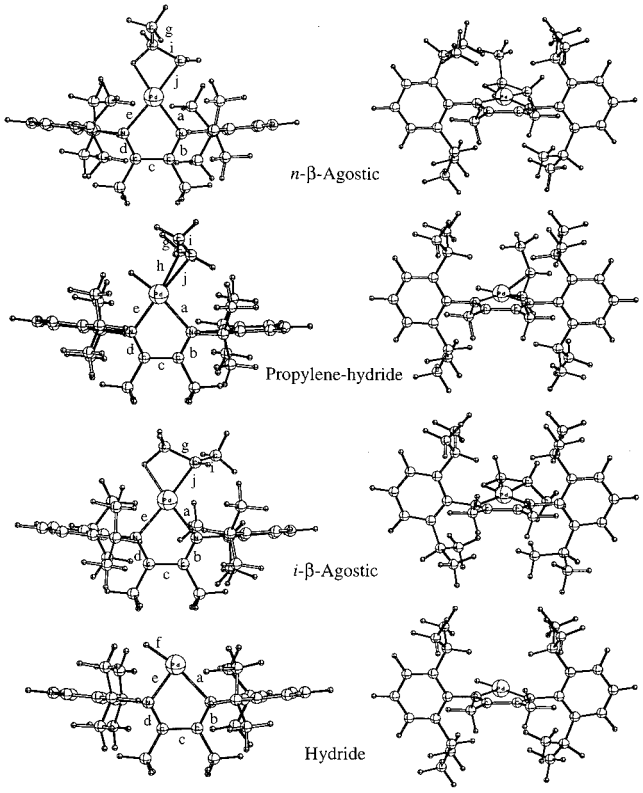

Figure 3. Two views of the structures of the *n*-β-agostic, propylene−hydride, the *i*-β-agostic, and metal−hydride intermediates in the β-H transfer process of ethylene polymerization with the substituted "real" diimine Ni and Pd catalysts. The structures depicted are for the Pd system at the IMOMM level. The distances of the labeled bonds are shown in Table 4.

Structure of the Real Catalysts. The optimized structures of the β-agostic *n*-propyl species, propylene−hydride intermediate, β-agostic isopropyl species, and the metal hydride for the substituted real catalytic systems are illustrated in Figure 3, with some important geometrical parameters for the model and real systems compared in Table 4. We focus on the geometrical differences between the model and real systems. For the β-agostic *n*-propyl species, which is the final point in the insertion reaction 1, there is little difference between the model and the real structures for both nickel and palladium catalysts. The most significant difference is the M−N bond length (e) trans to the M−C$^{\alpha}$ bond, which is shorter for the real system than the model system by 0.016 and 0.012 Å, for Ni and Pd, respectively.

For the propylene−hydride intermediate, there are more significant differences, as would be expected since the coordinating propylene is essentially perpendicular to the plane defined by the metal, hydride, and the imine groups, as in the methyl−ethylene π-complex discussed in the previous section. Furthermore, this species is more weakly bound, and the steric interactions likely play a larger role in affecting the geometries. For the nickel species, the Ni−C$^{\pi}$ bond lengths are 2.203 and 2.167 Å in the real system and 2.230 and 2.135 Å in the model system. For palladium, they are 2.274 and 2.330 Å in the real and 2.209 and 2.443 Å in the model system. It is interesting that substituent effects lead to a more symmetric π-complex. Typically, propylene π-complexes are quite asymmetric due to electronic effects of the methyl group, with the methyl-bearing carbon of propylene further away from the metal−ligands plane than the non-Me-bearing carbon. In this case, however, the

Table 4. Optimized Bond Lengths (Å) for the Structures in the β-H Transfer Process in Figure 3: *n*-β-Agostic, Propylene−Hydride, *i*-β-Agostic, and Metal Hydride Intermediates

		β-agostic *n*-propyl		olefin−hydride		β-agostic isopropyl		hydride	
		Ni	Pd	Ni	Pd	Ni	Pd	Ni	Pd
a	M−N	1.894 (1.889)	2.088 (2.078)	2.022 (2.013)	2.213 (2.175)	1.908 (1.891)	2.099 (2.088)	1.992 (2.004)	2.201 (2.206)
b	N═C	1.298 (1.293)	1.295 (1.289)	1.296 (1.290)	1.293 (1.289)	1.299 (1.292)	1.295 (1.289)	1.295 (1.289)	1.293 (1.288)
c	C−C	1.494 (1.479)	1.496 (1.480)	1.494 (1.482)	1.500 (1.479)	1.493 (1.479)	1.499 (1.481)	1.500 (1.485)	1.499 (1.483)
d	N═C	1.295 (1.292)	1.292 (1.288)	1.294 (1.291)	1.292 (1.290)	1.297 (1.292)	1.293 (1.287)	1.295 (1.291)	1.295 (1.290)
e	M−N	1.960 (1.976)	2.163 (2.175)	1.897 (1.906)	2.070 (2.073)	1.977 (1.983)	2.179 (2.190)	1.861 (1.863)	2.014 (2.019)
f	M−H					1.462 (1.463)	1.536 (1.534)		
g	C−Me	1.542 (1.542)	1.541 (1.542)	1.510 (1.507)	*1.510* (*1.511*)	1.507 (1.507)	1.503 (1.504)		
h	M−C			2.203 (2.230)	*2.330* (*2.443*)				
i	C−C	1.499 (1.499)	1.492 (1.495)	1.385 (1.386)	1.392 (1.399)	1.522 (1.523)	1.518 (1.520)		
j	M−C	1.911 (1.908)	2.062 (2.055)	2.167 (2.135)	2.274 (2.209)	1.928 (1.915)	2.074 (2.063)		

[a] For each species, the parameters are in the order of M = Ni for the real system and for the model system (in parentheses) and for M = Pd (in italics) for the real and the model system (in parentheses).

steric repulsion from the substituents on the aromatic diimine ligands pushes the Me-bearing carbon toward the metal−ligands plane, making the π-complex more symmetric. For the β-agostic isopropyl species, there are some differences between the real and model systems. The important one is the M−C bond length, which is slightly stretched by 0.013 (Ni) and 0.011 (Pd) Å in the real system. This increase is due to the steric repulsion between the substituents on the diimine ligands with the methyl group of isopropyl that is not involved in the agostic interaction.

Energetics for the Real Catalysts. This pathway is an important mechanism for polymer branching. For nickel, the energy of the olefin hydride "transition state" for the model catalyst was 13.6 kcal/mol above that for the β-agostic *n*-propyl species. The calculations for the real system, shown in Table 1, predict similar values of 14.5 (IMOMM) and 15.4 (MO// IMOMM) kcal/mol. Thus, this pathway is less likely for the real nickel catalyst.

For palladium, the model calculations suggested that branching could occur since the propylene hydride species was 5.4 kcal/mol above the β-agostic *n*-propyl species and the β-agostic isopropyl species (product) was 2.0 kcal/mol below the *n*-isomer (reactant). For the heavily substituted real system, the propylene hydride is now only 0.2 kcal/mol (−1.2 at the MO/IMOMM level) above the β-agostic *n*-propyl species, indicating that branching should occur more favorably for the heavily substituted Pd catalysts. Brookhart[4] has suggested that increasing the steric bulk of the diimine ligand leads to an increase in branching. This 5.2 kcal/mol difference between the model and real systems is mainly due to the 4.2 kcal/mol difference in the steric energy. If we compare the olefin hydride with the perpendicular π-complex, the larger steric energy associated with the olefin−alkyl system is understandable since there are a number of "close approaches" of ethylene with the MM substituents including one of 2.17 Å and one of 2.23 Å. The nearest two approaches in the propylene−hydride system are 2.29 and 2.44 Å. Due to the long-range interaction of the olefin−hydride species and the fact that the rotational potential energy surface is so flat, there is very little steric energy associated with the propylene−hydride, and in fact, it possesses 3.6 kcal/mol less steric energy than the reactants. Note that the propylene dissociation energy from β-agostic complex is reduced only by 3.5−4.0 kcal/mol upon going from the unsubstituted to the substituted system for Ni and Pd.

While it was found that the olefin−hydride species has decreased in energy relative to the *n*-β-agostic complex, especially for diimine−Pd complex, the *i*-β-agostic species, which is on the potential energy surface of the process starting from the olefin−hydride complex and leading to the branched polyethylene, has increased in energy due to steric interactions with substituents on the diimine ligand. In the case of nickel, the *i*-β-agostic species is now 6.5 kcal/mol higher in IMOMM energy than the *n*-β-agostic complex,while the previous model calculations had concluded that it resided 1.5 kcal/mol lower. Thus, for the nickel reaction, if the olefin−hydride intermediate could be accessed while an equilibrium is established between the two β-agostic species, the *n*-β-agostic species leading to linear polymers would be thermodynamically favored. For palladium, the situation is somewhat different. Model calculations showed that the *i*-β-agostic species was 2.0 kcal/mol lower in energy than the *n*-β-agostic intermediate, and although substituent effects retained the energetic order, it reduced to difference in IMOMM to only 0.5 kcal/mol. This difference in substituent effects between nickel and palladium can again be rationalized as due to smaller steric interactions associated with the larger palladium atom. With the reduced β-H transfer barrier in Pd, these two isomers are nearly thermoneutral with little kinetic barrier separating them, thus branching would be expected to be prominent in the palladium case. The extent of branching will be dependent on the diffusion-related barriers associated with olefin coordination in the propagation process.

In a separate paper, we will discuss the associative displacement chain termination process, which also starts from olefin−hydride complex.[8] It will be shown that, starting from the hydride, diimine−MH^+, the first ethylene binds to metal center by 35.9 kcal/mol, while the second one binds by 10.2 kcal/mol for nickel, and these numbers are 38.1 and 6.3 kcal/mol for palladium (unsubstituted model MO calculations).[8] Thus, if a 5-coordinate species was formed, an associative mechanism could be possible. However, it was shown that, for nickel, the barrier leading to the olefin−alkyl species (hydrogen transfer to an olefin) was much smaller than the 10.2 kcal/mol olefin dissociation limit; thus, associative displacement was not possible here. However, for palladium, the 6.3 kcal/mol required for dissociation of an ethylene is slightly lower than the activation barrier, 7.3 kcal/mol, for hydrogen migration leading to the olefin−alkyl species, indicating that an associative chain termination mechanism was possible as a chain termination process for palladium. When IMOMM calculations were performed, a stable 5-coordinate species was located for palladium, but it was higher in energy than the separated species, ethylene + ethylene−hydride complex. These data explained why substituted palladium polymerizes ethylene while an associative displacement mechanism prevents polymerization when the bulky substituents are not present.

5. Conclusions

The integrated molecular orbital−molecular mechanics (IMOMM) method has been used to study the real catalysts in the diimine−M (M = Ni, Pd) catalyzed ethylene polymerization reaction and compared with previous model MO calculations. For the insertion process, substituent effects lead to a lowering of the activation energy compared with model predictions. The activation barrier for nickel has been lowered from 9.9 kcal/mol (MO//model) to 3.8 (IMOMM) or 3.2 (MO//IMOMM) kcal/mol when substituents are taken into account. For palladium, the lowering of the model calculations is from 16.2 kcal/mol (MO//model) to 14.1 kcal/mol (IMOMM) or 13.9 (MO//IMOMM) kcal/mol. The substituents lead to steric interactions and an overall decrease in the complexation energy which leads to a lowering of the migratory insertion barrier.

The β-H transfer process which leads from the *n*-propyl β-agostic species to the olefin hydride intermediate to the isopropyl β-agostic complex is the likely mechanism leading to branching of polyethylenes. In the nickel system, model and real predictions would not change the qualitative picture that branching is unlikely in this case due to the height of the olefin−hydride intermediate. For palladium, where the olefin−hydride barrier was approximately 5.4 kcal/mol in model predictions, the IMOMM results reduce this difference and lead to almost no barrier which should suggest that branching is even more likely in the substituted case. This result qualitatively agrees with experiment which suggested that decreasing the steric bulk leads to more linear polymers.[4] The two β-agostic species which lead to linear and branched polymers by coordination of the next ethylene are thermodynamically almost equivalent in energy.

Very recently a theoretical paper on the related topics has been published by Ziegler and co-workers.[19] In an upcoming paper, we will discuss similarities and differences between our and their results in more details. However, in this paper, we briefly compare our present results with those of Ziegler et al.[19b] At first, we should note that, although we and Ziegler et al. used the same integrated MO + MM (IMOMM) approach developed in our group,[9] the methods used are different. In our calculations, we used the B3LYP/lanl2dz and MM3 methods for the "real" and "model" systems, respectively. Ziegler et al. used an DFT method including Vosko's local exchange-correlation functional together with Becke's nonlocal exchange and Perdew's nonlocal correlation functional for the "model" system, and AMBER95 force fields for the "real" system. In general, Ziegler et al.[19b] have found that the inclusion of bulky R and Ar ligands into calculations:

(a) destabilizes the diimine−Ni−olefin−alkyl π-complex by 5.3 kcal/mol, from 19.4 for the "model" to 14.7 kcal/mol for the "real" system;

(b) reduces the migratory insertion barrier by 4.3 kcal/mol, from 17.5 to 13.2 kcal/mol;

(c) slightly increases the chain isomerization barrier, from 12.8 to 15.3 kcal/mol, and

(d) slightly decreases the exothermicity of the chain isomerization reaction, from 1.8 to 0.8 kcal/mol.

According to our calculations, shown in Table 1, upon inclusion of bulky R and Ar ligands:

(a) the diimine−Ni−olefin−alkyl π-complex is destabilized by 7.5 kcal/mol, from 27.9 for the "model" to 20.4 kcal/mol for the "real" system;

(b) the migratory insertion barrier is lowered by 5.7 kcal/mol, from 9.9 to 3.2 kcal/mol;

(c) the chain isomerization barrier is increased by 0.9 kcal/mol, from 13.6 to 14.5 kcal/mol;

(d) the exothermicity of the chain isomerization process is decreased by 8.0 kcal/mol from −1.5 to 6.5 kcal/mol, and as a result, this process becomes endothermic by 6.5 kcal/mol.

A comparison our results obtained in the present paper with those of Ziegler et al.[19b] shows that they are very similar with exception of the decrease in exothermicity of the chain isomerization reaction, which can be due to different methods. The detail of the differences will be discussed in an upcoming paper.

Acknowledgment. The use of the computational facilities and programs at the Emerson Center is acknowledged. The present research is in part supported by grants (CHE-9409020 and CHE-9627775) from the National Science Foundation. R.D.J.F. acknowledges a Postdoctoral Fellowship from the Natural Sciences and Engineering Research Council of Canada.

JA9728334

(19) (a) Deng, L.; Margl, P.; Ziegler, T. *J. Am. Chem. Soc.* **1997**, *119*, 1094. (b) Deng L.; Woo, T. K.; Cavallo, L.; Margl, P M.; Ziegler T. *J. Am. Chem. Soc.* **1997**, *119*, 6177.